Modeling The Full-Bridge Series-Resonant Power Converter

R.J. KING

T.A. STUART, Senior Member, IEEE
University of Toledo

A steady state model is derived for the full-bridge series-resonant power converter. Normalized parametric curves for various currents and voltages are then plotted versus the triggering angle of the switching devices. The calculations are compared with experimental measurements made on a 50 kHz converter and a discussion of certain operating problems is presented.

Manuscript received August 28, 1981.

This work was supported by the National Aeronautics and Space Administration Lewis Research Center under Grant NSG-3281.

Authors' address: Department of Electrical Engineering, University of Toledo, 2801 West Bancroft St., Toledo, OH 43606.

0018-9251/82/0700-0449 $00.75

INTRODUCTION

The present state of the art in power electronics offers a wide variety of options to the power supply design engineer. Several different varieties of high power switching circuits are now available, each with its own particular advantages and characteristics. One of these circuits which has generated considerable interest is the series resonant converter, which has been widely used in dc power supplies in both half- and full-bridge configurations. The low weight and high efficiency advantages of this circuit have made it especially popular in the aerospace industry, where these characteristics are of utmost importance.

Although series-resonant converters are widely used in aerospace systems, certain characteristics of these circuits are still not widely understood by design engineers. This leads to a number of problems in their application, many of which can be traced to the lack of straightforward models. In an effort to overcome this difficulty, an earlier paper [1] proposed a normalized model for the half-bridge version of this circuit. This model included derivations for the more important steady state circuit equations and presented several of the results in a normalized graphical form. Due to the success of this approach, it was decided to extend this analysis to the full-bridge converter so that complete models would be available for both versions.

Both the half- and full-bridge converters have been studied in several references [1-8] and the relative merits of the two are well known. Perhaps the most important advantage of the full bridge is that the load voltage V_0 in Fig. 1 can approach (although never quite reach) the source voltage V_s. This is in contrast to the half bridge where V_0 can only approach 0.5 V_s. In other words, the full-bridge circuit must switch only half as much current for fixed values of V_s and output power. This means that the necessary volt-ampere product for the full-bridge switching devices is only half of that required by the half bridge. Because of this advantage, the full bridge will be the preferred configuration for many applications.

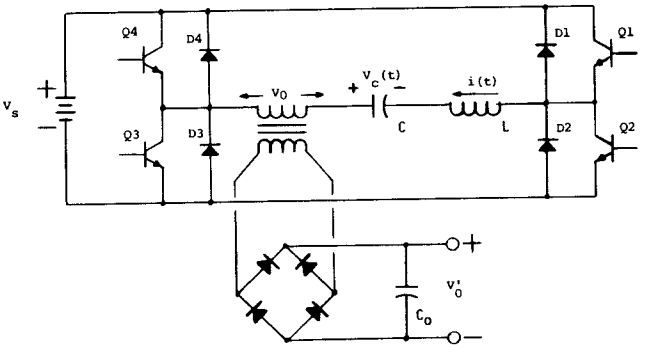

Fig. 1. Basic schematic of full-bridge series resonant converter. The polarity of V_0 is such that it always opposes the current in the transformer primary.

The half-bridge converter has been analyzed in detail in [1, 2, 5] and the full-bridge characteristics have been previously considered in [7]. This analysis builds on these earlier studies to present a more complete derivation of the full-bridge model. There are similarities between the half- and full-bridge equations, but these similarities are not always obvious, and important differences also exist. Therefore, to avoid ambiguity, it is necessary to present the complete derivations for most of the full-bridge equations. Analyses are included for both the continuous and discontinuous steady state operating modes, and certain results are presented in the form of normalized graphs. Test results for a 50 kHz converter are included to provide experimental verification.

NOMENCLATURE

A, B	Terms defined by (15) and (16).
C	Resonance capacitor.
E_L	Energy supplied to load.
E_S	Energy obtained from source.
I_{avg}	Half-cycle average output current at primary of transformer.
$I_{D\,avg}$	Average diode current.
I_0	i at $t = 0$.
I_2	i at $t = t_2$.
I_{peak}	Peak value of output current at primary of transformer.
$I_{Q\,avg}$	Average transistor current.
I_{rms}	RMS output current at primary of transformer.
$i(t)$	Output current at primary of transformer.
L	Resonance inductor.
q	Normalized load voltage defined by (2).
$V_{c\,peak}$	Peak capacitor voltage.
$v_c(t)$	Voltage across C.
V_{Ci}	Voltage across capacitor at time t_i.
V_0	Amplitude of square-wave output voltage at primary of transformer. V_0 is always considered positive.
V_0	DC load voltage.
V_s	DC source voltage.
Z_0	Characteristic impedance defined by (2).
α	Delay angle.
β	Transistor conduction angle.
w_0	Resonance frequency (in radians per second) defined by (2).

CONTINUOUS CURRENT OPERATION

The schematic of a full-bridge converter is shown in Fig. 1. The circuit shown here is very fundamental and does not include any of the auxiliary circuitry required for $Q1 - Q4$. Bipolar transistors are shown for the switching devices, but since the analysis assumes an ideal switch, it is equally valid for silicon controlled rectifiers (SCRs) or power metal-oxide semiconductor field-effect transistors (MOSFETs). The ideal load current waveform for continuous operation is shown in Fig. 2.

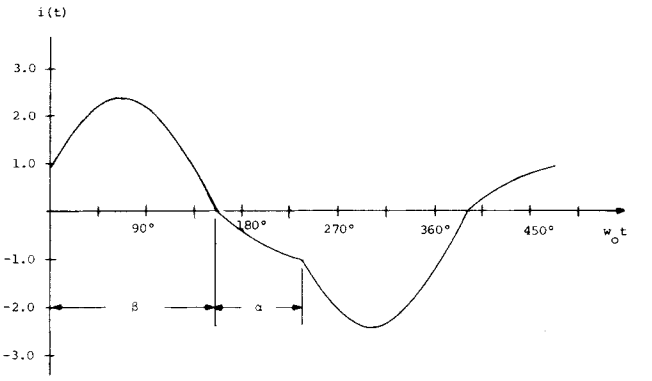

Fig. 2. Typical normalized load current waveform in continuous current operation $q = 0.7$, $\alpha = 80°$, $\beta = 156°$).

As for the half-bridge model discussed in [1], this analysis is based on certain approximations. The first of these is that the output voltage V_0 is constant. This implies that the transformer primary voltage V_0 is equivalent to a dc source that changes polarity so that it always opposes the primary current. The second approximation is that all circuit components are ideal, i.e., turn-on and turn-off times are ignored and the components are assumed to be lossless. In practice the lossless approximation can be reconciled with the actual circuit simply by adding the circuit losses to the load.

The basic operation of the circuit can be determined by referring to Figs. 1 and 2. If Q_1 and Q_3 are turned on at $t = 0$, $i(t)$ will resonate first in the positive direction and then in the negative position through D_1 and D_3. At some time t_2 during this negative interval, Q_2 and Q_4 are turned on and $i(t)$ transfers from $D_1 - D_3$ to $Q_2 - Q_4$. The current continues to resonate first in the negative direction and then in the positive direction through D_2 and D_4. The energy transferred to the load is controlled by varying the times at which $Q_1 - Q_3$ and $Q_2 - Q_4$ are turned on.

We define the terms

$$V_{c0} \equiv v_c(0); \quad V_{c1} \equiv v_c(t_1); \quad V_{c2} \equiv v_c(t_2) \tag{1}$$

$$w_0 \equiv 1/\sqrt{LC}; \quad z_0 \equiv \sqrt{L/C}; \quad q \equiv V_0/V_s \tag{2}$$

$$\alpha \equiv w_0(t_2 - t_1)$$

$$\beta \equiv w_0 t_1, \qquad t' \equiv t - t_1. \tag{3}$$

where $\alpha \leqslant 180°$ for continuous conduction.

If $Q1$ and $Q3$ are turned on at $t = 0$ ($Q2$ and $Q4$ are turned on at t_2) and

$$i(0) \equiv I_0 \tag{4}$$

we have

$$i(t) = I_0 \cos(w_0 t) + [(V_{c0} + V_s - V_0)/Z_0] \sin(w_0 t), \quad 0 \leqslant t \leqslant t_1 \tag{5}$$

$$i(t') = [(V_{c1} + V_s + V_0)/Z_0] \sin(w_0 t'), \quad 0 \leqslant t' \leqslant t_2 - t_1. \tag{6}$$

Since $i(t) = 0$ at $w_0 t = \beta$, where $\beta > 0$, we have from (5),

$$\beta \equiv w_0 t_1 = \tan^{-1}[-I_0 Z_0/(V_{c0} + V_s - V_0)] + \pi. \tag{7}$$

For the capacitor voltage we have

$$\begin{aligned} v_c(t) &= V_{c0} + (1/C) \int_0^t - i(t)\, dt \qquad 0 \leqslant t \leqslant t_1 \\ &= - I_0 Z_0 \sin(w_0 t) + (V_{c0} + V_s - V_0) \\ &\quad \cdot \cos(w_0 t) + V_0 - V_s. \end{aligned} \tag{8}$$

Therefore

$$\begin{aligned} V_{c1} = v_c(t_1) &= - I_0 Z_0 \sin\beta + (V_{c0} + V_s - V_0) \\ &\quad \cdot \cos\beta + V_0 - V_s. \end{aligned} \tag{9}$$

Likewise

$$\begin{aligned} v_c(t') &= V_{c1} + (1/C) \int_0^{t'} - i(t')\, dt', \\ &\quad \cdot 0 \leqslant t' \leqslant t_2 - t_1 \\ &= (V_{c1} + V_s + V_0) \cos(w_0 t') - V_0 - V_s. \end{aligned} \tag{10}$$

Therefore

$$\begin{aligned} V_{c2} = v_c(t' = t_2 - t_1) &= (V_{c1} + V_s + V_0) \\ &\quad \cdot \cos\alpha - V_0 - V_s. \end{aligned} \tag{11}$$

For cyclic stability, the conditions at t_2 must be symmetric with those at $t = 0$; therefore

$$V_{c2} = - V_{c0} \quad \text{and} \quad i(t_2) \equiv I_2 = -I_0. \tag{12}$$

The energy into the load during $0 \leqslant t \leqslant t_2$ is given by the following expressions:

$$\begin{aligned} E_{L1} &= |V_0| \int_0^{t_1} i(t)\, dt \\ &= (V_0/w_0) \{I_0 \sin\beta + [(V_{c0} + V_s - V_0)/Z_0] \\ &\quad \cdot (1 - \cos\beta)\} \end{aligned} \tag{13}$$

$$\begin{aligned} E_{L2} &= -|V_0| \int_0^{t_2 - t_1} i(t')\, dt', \\ &\quad (i(t) \text{ changes direction}) \\ &= (V_0/w_0)(1 - \cos\alpha) \{I_0 \sin\beta \\ &\quad - [(V_{c0} + V_s - V_0)/Z_0] \cos\beta - 2V_0/Z_0\}. \end{aligned} \tag{14}$$

Defining the following terms

$$A \equiv \{I_0 \sin\beta + [(V_{c0} + V_s - V_0)/Z_0](1 - \cos\beta)\} \tag{15}$$

$$\begin{aligned} B &\equiv (1 - \cos\alpha) \{I_0 \sin\beta - [(V_{c0} + V_s - V_0)/Z_0] \\ &\quad \cdot \cos\beta - 2V_0/Z_0\} \\ &= (1 - \cos\alpha)[A - (V_{c0} + V_s + V_0)/Z_0] \end{aligned} \tag{16}$$

the total energy into the load during the interval $0 \leqslant t \leqslant t_2$ is

$$E_L \equiv E_{L1} + E_{L2} = (|V_0|/w_0)(A + B). \tag{17}$$

The energy from the source V_s is given by the following expressions:

$$E_{S1} = V_s \int_0^{t_1} i(t)\, dt = V_s A/w_0 \tag{18}$$

$$E_{S2} = V_s \int_0^{t_2 - t_1} i(t')\, dt' = - V_s B/w_0. \tag{19}$$

Therefore the total energy from V_s during the interval $0 \leqslant t \leqslant t_2$ is

$$E_S = (V_s/w_0)(A - B). \tag{20}$$

The energy stored in the circuit elements at t_0 is given by

$$E_{ST0} = \tfrac{1}{2} L I_0^2 + \tfrac{1}{2} C V_{c0}^2. \tag{21}$$

The energy stored in the circuit elements at t_2 is given by

$$E_{ST2} = \tfrac{1}{2} L I_2^2 + \tfrac{1}{2} C V_{c2}^2. \tag{22}$$

Substituting from (12),

$$E_{ST2} = \tfrac{1}{2} L (-I_0)^2 + \tfrac{1}{2} C(-V_{c0})^2$$

or

$$E_{ST0} = E_{ST2}. \tag{23}$$

Since the stored energy is the same at t_0 and t_2, and the circuit components are assumed to be ideal,

$$E_S = E_L. \tag{24}$$

Therefore

$$(V_s/w_0)(A - B) = (V_0/w_0)(A + B) \tag{25}$$

or

$$q \equiv V_0/V_s = (A - B)/(A + B) \tag{26}$$

and

$$B/A = (1 - q)/(1 + q). \tag{27}$$

We now consider the capacitor voltage relationships. From (9) and (15),

$$V_{c1} = V_{c0} - A\,Z_0. \tag{28}$$

From (11) and (28),

$$\begin{aligned} V_{c2} &= (V_{c0} + V_s - A\,Z_0 + V_0)\cos\alpha - V_0 - V_s \\ &= Z_0(1 - \cos\alpha)[A - (V_{c0} + V_s + V_0)/Z_0] \\ &\quad + V_{c0} - A\,Z_0. \end{aligned} \tag{29}$$

From (16) and (29),

$$V_{c2} = B\,Z_0 - A\,Z_0 + V_{c0}. \tag{30}$$

For cyclic stability,

$$V_{c2} = -V_{c0}. \tag{31}$$

From (30) and (31),

$$V_{c0} = (Z_0/2)(A - B). \tag{32}$$

From (27) and (32),

$$V_{c0} = A\,Z_0[q/(1 + q)]. \tag{33}$$

From (28) and (33),

$$V_{c1} = -A\,Z_0[1/(1 + q)]. \tag{34}$$

Repeating (16),

$$B = (1 - \cos\alpha)[A - (V_{c0} + V_s + V_0)/Z_0]. \tag{35}$$

Therefore

$$\begin{aligned} \cos\alpha &= [A - B - (V_{c0} + V_s + V_0)/Z_0]/ \\ &\quad [A - (V_{c0} + V_s + V_0)/Z_0]. \end{aligned} \tag{36}$$

From (27), (33), and (36),

$$\begin{aligned} \cos\alpha &= \big(2Aq/(1 + q) - \{A\,Z_0[q/(1 + q)] + V_0 \\ &\quad + V_s\}(1/Z_0)\big)/\big(A - \{A\,Z_0[q/(1 + q)] + V_0 \\ &\quad + V_s\}(1/Z_0)\big). \end{aligned} \tag{37}$$

Substituting $V_0 = V_s q$,

$$\begin{aligned} \cos\alpha &= [A\,q - (V_s/Z_0)(1 + q)^2]/ \\ &\quad [A - (V_s/Z_0)(1 + q)^2] \end{aligned} \tag{38}$$

or

$$A = (V_s/Z_0)[(1 + q)^2(1 - \cos\alpha)/(q - \cos\alpha)]. \tag{39}$$

Substituting (39) into (33) and (34) produces,

$$V_{c0} = V_s[q(1 + q)(1 - \cos\alpha)/(q - \cos\alpha)] \tag{40}$$

$$V_{c1} = V_s[-(1 + q)(1 - \cos\alpha)/(q - \cos\alpha)]. \tag{41}$$

For cyclic stability,

$$I_0 = -I_2. \tag{42}$$

Therefore from (4), (6), and (42),

$$-I_0 = [(V_s + V_{c1} + V_0)/Z_0]\sin w_0(t_2 - t_1). \tag{43}$$

Substituting for V_{c1} from (41),

$$I_0 = (V_s/Z_0)[(1 - q^2)\sin\alpha/(q - \cos\alpha)]. \tag{44}$$

From (2), (7), (40), and (44),

$$\begin{aligned} \beta &= \pi + \tan^{-1}\{(q^2 - 1)\sin\alpha/ \\ &\quad [2q - (1 + q^2)\cos\alpha]\}. \end{aligned} \tag{45}$$

We can now determine the average rectified value of $i(t)$,

$$\begin{aligned} I_{\text{avg}} &= (1/t_2)\Big(\int_0^{t_1} \{I_0\cos(w_0 t) \\ &\quad + [(V_{c0} + V_s - V_0)/Z_0]\sin(w_0 t)\}dt \\ &\quad - \int_0^{t_2 - t_1} [(V_{c1} + V_s + V_0)/Z_0]\sin(w_0 t')\,dt'\Big) \\ &= (1/w_0 t_2)\{I_0\sin\beta - [(V_{c0} + V_s - V_0)/Z_0] \\ &\quad \cdot(\cos\beta - 1) \\ &\quad + [(V_{c1} + V_s + V_0)/Z_0](\cos\alpha - 1)\}. \end{aligned} \tag{46}$$

Substituting the value of V_{c1} from (9) into (46) yields

$$I_{avg} = (1/w_0 t_2)(I_0 \sin\beta - [(V_{c0} + V_s - V_0)/Z_0] \cdot (\cos\beta - 1) + (1 - \cos\alpha)\{-2V_0/Z_0 + I_0 \sin\beta - [(V_{c0} + V_s - V_0)/Z_0]\cos\beta\}). \quad (47)$$

Comparing (47) with (15) and (16) we have

$$I_{avg} = (A + B)/w_0 t_2. \quad (48)$$

From (27),

$$B = A\,[(1 - q)/(1 + q)]. \quad (49)$$

Therefore

$$I_{avg} = 2A/[(\alpha + \beta)(1 + q)]. \quad (50)$$

From (34) and (50),

$$I_{avg} = (V_s/Z_0)[2(1 + q)(1 - \cos\alpha)/(\alpha + \beta)(q - \cos\alpha)]. \quad (51)$$

To determine the peak value of $i(t)$, we differentiate (5) and set the result = 0,

$$d\,i(t)/dt = -w_0 I_0 \sin(w_0 t) + w_0 \cdot [(V_{c0} + V_s - V_0)/Z_0]\cos(w_0 t) = 0. \quad (52)$$

Therefore

$$I_{peak} \text{ occurs at } w_0 t_{max} = \tan^{-1} \cdot [(V_{c0} + V_s - V_0)/I_0 Z_0] \quad (53)$$

but from (7),

$$\beta - \pi = \tan^{-1}[-I_0 Z_0/(V_{c0} + V_s - V_0)] \quad (54)$$

and

$$w_0 t_{max} = \beta - \pi/2 \quad (55)$$

$$I_{peak} = I_0 \sin\beta - [(V_{c0} + V_s - V_0)/Z_0]\cos\beta. \quad (56)$$

Comparing (15) and (57),

$$I_{peak} = A - (V_{c0} + V_s - V_0)/Z_0. \quad (57)$$

Substituting (39), (40), and $V_0 = qV_s$ into (58),

$$I_{peak} = (V_s/Z_0)[(1 + q^2 - 2q\cos\alpha)/(q - \cos\alpha)]. \quad (58)$$

For the rms value of $i(t)$ we have

$$I_{rms} = \left[(1/t_2)\left(\int_0^{t_1}\{I_0 \cos w_0 t + [(V_{c0} + V_s - V_0)/Z_0]\sin w_0 t\}^2 dt + \int_0^{t_2 - t_1}\{[(V_{c1} + V_s + V_0)/Z_0]\sin w_0 t'\}^2 dt'\right)\right]^{1/2} \quad (59)$$

$$I_{rms} = \Big([1/(\alpha + \beta)]\{I_0^2(\beta/2 + \sin 2\beta/4) + [(V_{c0} + V_s - V_0)/Z_0]^2(\beta/2 - \sin 2\beta/4) + [I_0(V_{c0} + V_s - V_0)/Z_0]\sin^2\beta + [(V_{c1} + V_s + V_0)/Z_0]^2 \cdot (\alpha/2 - \sin 2\alpha/4)\}\Big)^{1/2}. \quad (60)$$

By integrating and substituting as in (46) and (47) we also can obtain the average transistor current $I_{Q\,avg}$ and the average diode current $I_{D\,avg}$

$$I_{Q\,avg} = A/2(\alpha + \beta) \quad (61)$$

$$I_{D\,avg} = B/2(\alpha + \beta). \quad (62)$$

Substituting (39) for A, (45) for β, and (49) for B,

$$I_{Q\,avg} = (V_s/Z_0)[(1 + q)^2(1 - \cos\alpha)/2(q - \cos\alpha) \cdot (\alpha + \beta)] \quad (63)$$

$$I_{D\,avg} = (V_s/Z_0)[(1 - q^2)(1 - \cos\alpha)/2(q - \cos\alpha) \cdot (\alpha + \beta)]. \quad (64)$$

Another variable of interest is the peak capacitor voltage. From Figs. 1 and 2 it can be seen that the peak voltage across C will occur at $t = t_1$ and at $t = t_3$ where $i(t)$ reverses. Therefore from (41),

$$V_{c\,peak} = \pm V_{c1} = \pm V_s \cdot \{[(1 + q)(1 - \cos\alpha)]/(q - \cos\alpha)\}. \quad (65)$$

In [1] it was established that for the half-bridge circuit,

$$\cos^{-1} q < \alpha \leqslant 180° \quad (66)$$

for continuous current, steady state operation, and that

$$1 \geqslant q > \cos\alpha. \quad (67)$$

By using a procedure exactly the same as in [1], it can be established that (66) and (67) also apply for the full-bridge case.

DISCONTINUOUS CURRENT OPERATION

The discontinuous output current waveform for some $\alpha > 180°$ is shown in Fig. 3. All approximations are identical to the continuous current analysis.

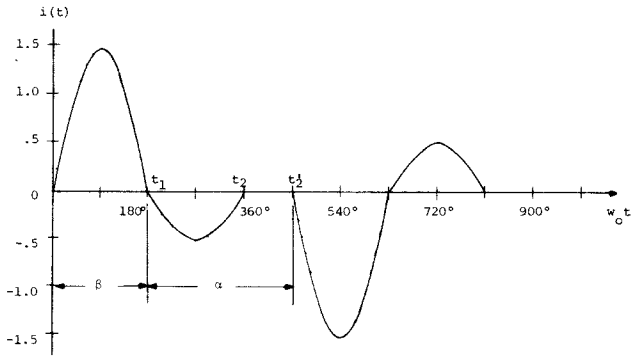

Fig. 3. Typical normalized load current waveform in discontinuous current operation ($q = 0.5$, $\alpha = 270°$, $\beta = 160°$).

If $Q1$ and $Q3$ are turned on at $t = 0$,

$$i(t) = [(V_{10} + V_s - V_0)/Z_0] \sin(w_0 t), \quad 0 \leqslant t \leqslant t_1 \tag{68}$$

$$i(t') = [(V_{11} + V_s + V_0)/Z_0] \sin(w_0 t'), \quad 0 \leqslant t' \leqslant t_2 - t_1 \tag{69}$$

$$i(t) = 0, \quad t_2 \leqslant t \leqslant t_2' \tag{70}$$

where in this case we have

$$I_0 = 0 \tag{71}$$

$$w_0 t_1 = w_0(t_2 - t_1) = \pi \tag{72}$$

$$\alpha \equiv w_0(t_2' - t_1), \quad \beta = \pi. \tag{73}$$

By comparison with the continuous current analysis, we see that all calculations will be virtually the same except that different time intervals will be used for the average and rms currents. Therefore most of the previous calculations can be extended to the discontinuous case.

From (15) and (16), replacing the α in these expressions with π,

$$A = 2(V_{c0} + V_s - V_0)/Z_0 \tag{74}$$

$$B = 2(V_{c0} + V_s - 3V_0)/Z_0. \tag{75}$$

From (40) and (41), replacing the α in these expressions with π,

$$V_{c0} = 2V_s q \tag{76}$$

$$V_{c1} = -2V_s. \tag{77}$$

Using an approach similar to (46),

$$I_{avg} = (1/w_0 t_2')[(2V_{c0} - 2V_{c1} - 4V_0)/Z_0] = (V_s/Z_0)[4/(\alpha + \pi)]. \tag{78}$$

From (58),

$$I_{peak} = [V_s(1 + q)]/Z_0. \tag{79}$$

Using an approach similar to (59) and (60),

$$I_{rms} = ((1/w_0 t_2')\{[(V_{c0} + V_s - V_0)/Z_0]^2 (\pi/2) + [(V_{c1} + V_s + V_0)/Z_0]^2(\pi/2)\})^{1/2} = (V_s/Z_0)[(1 + q^2)\pi/(\alpha + \pi)]^{1/2}. \tag{80}$$

From (61) and (62),

$$I_{Q\,avg} = V_s(1 + q)/Z_0(\alpha + \pi) \tag{81}$$

$$I_{D\,avg} = V_s(1 - q)/Z_0(\alpha + \pi) \tag{82}$$

and from (65),

$$V_{c\,peak} = 2V_s. \tag{83}$$

SUMMARY OF EQUATIONS AND NORMALIZED CURVES

The final equations are summarized in Tables I and II along with the results for the half-bridge configuration reported in [1]. This provides a handy reference and indicates some of the key differences between the two circuits.

From a circuit design standpoint, those variables of most importance might be I_{avg}, I_{peak}, I_{rms}, $V_{c\,peak}$, $I_{Q\,avg}$, and $I_{D\,avg}$. These variables are of particular interest since they help determine the necessary ratings for the components in Fig. 1. As suggested in [1], these variables can be presented in a more convenient form if they are plotted on normalized curves. This is accomplished by defining the following base quantities:

$$I_{base} = V_s/Z_0 \tag{84}$$

$$V_{base} = V_s. \tag{85}$$

The actual current I or voltage V is then divided by the base quantity to produce normalized values,

$$\text{normalized current} = I_n = I/I_{base} \tag{86}$$

$$\text{normalized voltage} = V_n = V/V_{base}. \tag{87}$$

TABLE I

Comparison of Key Voltages and Currents for Half-Bridge and Full-Bridge Configurations in Steady State Continuous Current Operation

Continuous Current

$\cos^{-1} q < \alpha \leqslant \pi; \qquad \beta = \pi + \tan^{-1}\{-(1 - q^2)\sin\alpha/[2q - (1 + q^2)\cos\alpha]\}$

Half Bridge	Full Bridge
$I_0 = (V_s/2Z_0)[(1 - q^2)\sin\alpha/(q - \cos\alpha)]$	$I_0 = (V_s/Z_0)[(1 - q^2)\sin\alpha/(q - \cos\alpha)]$
$I_{avg} = (V_s/2Z_0)[2(1 + q)(1 - \cos\alpha)/(\alpha + \beta)(q - \cos\alpha)]$	$I_{avg} = (V_s/Z_0)[2(1 + q)(1 - \cos\alpha)/(\alpha + \beta)(q - \cos\alpha)]$
$I_{peak} = (V_s/2Z_0)[(1 + q^2 - 2q\cos\alpha)/(q - \cos\alpha)]$	$I_{peak} = (V_s/Z_0)[(1 + q^2 - 2q\cos\alpha)/(q - \cos\alpha)]$
$I_{rms} = \{[1/(\alpha + \beta)][I_0^2(\beta/2 + \sin2\beta/4) + [(V_{c0} - V_0)/Z_0]^2(\beta/2 - \sin2\beta/4) + I_0[(V_{c0} - V_0)/Z_0]\sin^2\beta + [(V_{c1} + V_0)/Z_0]^2(\alpha/2 - \sin2\alpha/4)]\}^{1/2}$	$I_{rms} = \{[1/(\alpha + \beta)][I_0^2(\beta/2 + \sin2\beta/4) + [(V_{c0} + V_s - V_0)/Z_0]^2(\beta/2 - \sin2\beta/4) + I_0[(V_{c0} + V_s - V_0)/Z_0]\sin^2\beta + [(V_{c1} + V_s + V_0)/Z_0]^2(\alpha/2 - \sin2\alpha/4)]\}^{1/2}$
$I_{Q\,avg} = [(1 + q)/4]\, I_{avg}$	$I_{Q\,avg} = [(1 + q)/4]\, I_{avg}$
$I_{D\,avg} = [(1 - q)/4]\, I_{avg}$	$I_{D\,avg} = [(1 - q)/4]\, I_{avg}$
$V_{c0} = (V_s/2)[1 + q(1 + q)(1 - \cos\alpha)/(q - \cos\alpha)]$	$V_{c0} = V_s[q(1 + q)(1 - \cos\alpha)/(q - \cos\alpha)]$
$V_{c1} = (V_s/2)[1 - (1 + q)(1 - \cos\alpha)/(q - \cos\alpha)]$	$V_{c1} = V_s[-(1 + q)(1 - \cos\alpha)/(q - \cos\alpha)]$
$V_{c\,peak} = (V_s/2)[1 + (1 + q)(1 - \cos\alpha)/(q - \cos\alpha)]$	$V_{c\,peak} = V_s[\pm(1 + q)(1 - \cos\alpha)/(q - \cos\alpha)]$
$q \equiv 2V_0/V_s$	$q \equiv V_0/V_s$

TABLE II

Comparison of Key Voltages and Currents for Half-Bridge and Full-Bridge Configurations in Steady State Discontinuous Current Operation

Discontinuous Current

$\alpha \geqslant \pi; \qquad \beta = \pi$

Half Bridge	Full Bridge
$I_0 = 0$	$I_0 = 0$
$I_{avg} = (V_s/2\,Z_0)[4/(\alpha + \pi)]$	$I_{avg} = (V_s/Z_0)[4/(\alpha + \pi)]$
$I_{peak} = (V_s/2Z_0)(1 + q)$	$I_{peak} = (V_s/Z_0)(1 + q)$
$I_{rms} = (V_s/2Z_0)[(1 + q^2)\pi/(\alpha + \pi)]^{1/2}$	$I_{rms} = (V_s/Z_0)[(1 + q^2)\pi/(\alpha + \pi)]^{1/2}$
$I_{Q\,avg} = [(1 + q)/4]\, I_{avg}$	$I_{Q\,avg} = [(1 + q)/4]\, I_{avg}$
$I_{D\,avg} = [(1 - q)/4]\, I_{avg}$	$I_{D\,avg} = [(1 - q)/4]\, I_{avg}$
$V_{c0} = (V_s/2)(1 + 2q)$	$V_{c0} = V_s(2q)$
$V_{c1} = (V_s/2)(-1)$	$V_{c1} = V_s(-2)$
$V_{c\,peak} = (V_s/2)(3)$	$V_{c\,peak} = V_s = V_s(\pm 2)$

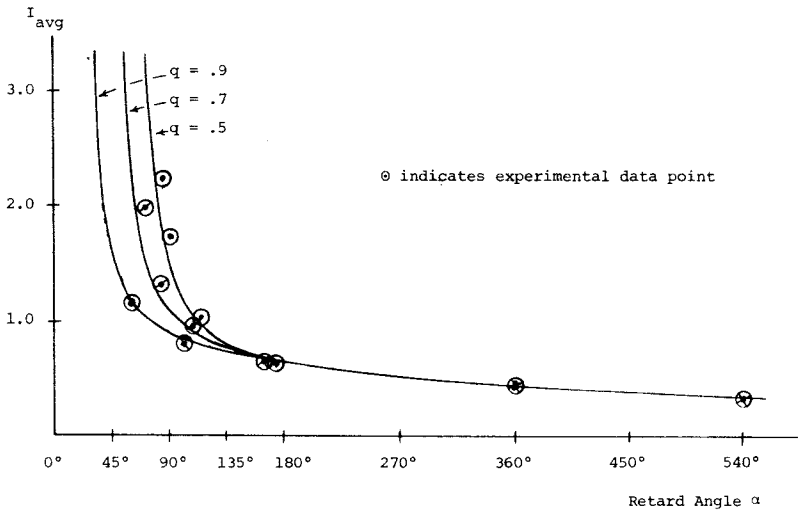

Fig. 4. Normalized average load current versus retard angle α with normalized load voltage as parameter.

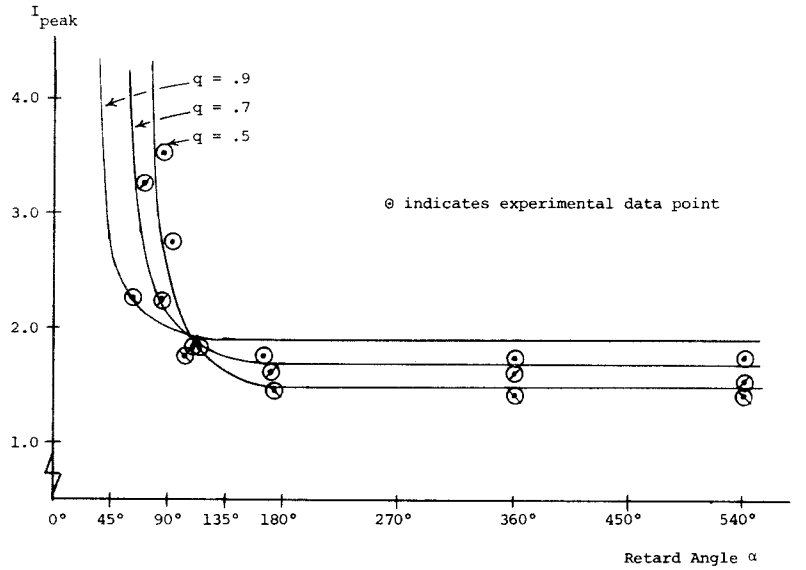

Fig. 5. Normalized peak load current versus retard angle α with normalized load voltage as parameter.

The approach is analogous to the familiar "per unit" system that is commonly used in the analysis of large electric power grids.

Figs. 4 to 7 show the normalized curves for I_{avg}, I_{peak}, I_{rms}, and $V_{c\,peak}$ versus the retard angle α for various values of q. The discrete points on the curves indicate experimental data taken from a 50 kHz converter. These experimental results are discussed in the following section.

EXPERIMENTAL RESULTS

In order to evaluate the accuracy of the previous analysis, a small full-bridge converter was built and tested. This converter had the following ratings and parameters:

$$V_s = 150 \text{ Vdc}; \quad f_0 = 50 \text{ kHz}; \quad Z_0 = 196\Omega$$

$$P_{out} = 150 \text{ W(maximum)}.$$

Waveforms of the load current $i(t)$ and the current in one of the transistor-diode pairs (e.g. $Q1$-$D1$) are shown in Fig. 8. As seen from Figs. 4-7, the calculated and experimental results are in reasonable agreement. However the deviations between the two are somewhat greater than those reported earlier in [1] for the half-

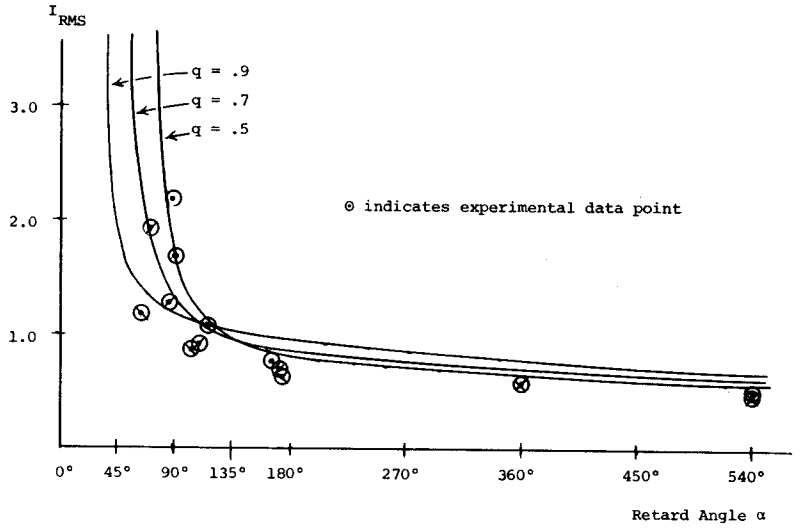

Fig. 6. Normalized rms load current versus retard angle α with normalized load voltage as parameter.

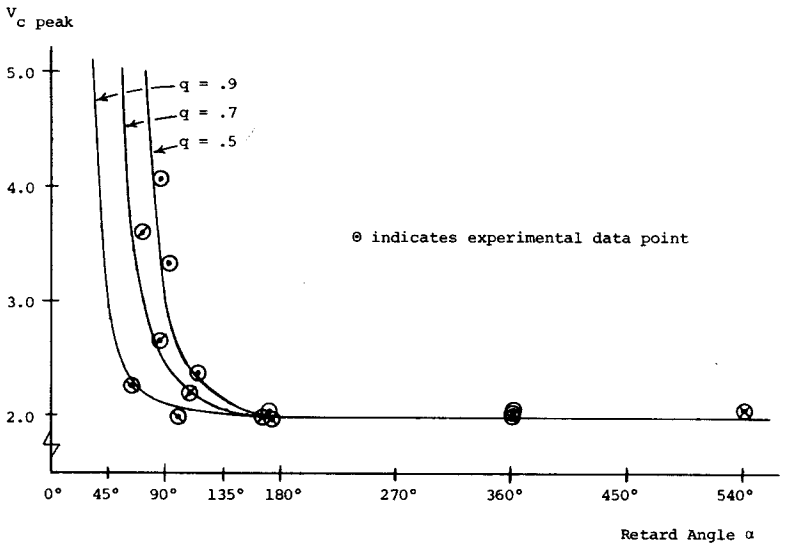

Fig. 7. Normalized peak capacitor voltage versus retard angle α with normalized load voltage as parameter.

bridge converter. The main reason for these larger errors is probably related to the higher resonant frequency of the full-bridge circuit (50 kHz) for the full bridge, 10 kHz for the half-bridge). This higher frequency induces higher parasitic losses in the various components, and slightly increases the errors in measuring the various time intervals on the oscilloscope. All circuit losses were lumped with the output power by using the same procedure described in [1] for the half-bridge circuit. Also as in [1], the output transformer shown in Fig. 1 was omitted from the actual circuit in order to further reduce the losses and simplify the control circuitry.

The actual circuit also included a refinement referred to as a "commutating circuit" which was connected in series with each transistor as shown in Fig. 9. The purpose of this circuit was to reduce the transistor turn-on losses which can occur in the continuous current mode. Without these commutating circuits additional transistor turn-on switching loss can occur in the following manner. Referring to the schematic in Fig. 9 and the waveforms in Fig. 10, $Q2$ starts to turn on while $D1$ is still conducting (i.e., $i(t) = i_{D1} + i_{c2} = I_{01}$ and is essentially constant during the switching interval). Since the i_{c2} rise time is finite, i_{c2} will gradually rise to the level of I_{01} in about 200 ns and then draw a brief transient overshoot current until $D1$ recovers (approximately an additional 300 ns). Since $D1$ remains on for most of this total 500 ns interval, v_{CE2} of $Q2$ is clamped at V_s while i_{c2} continues to rise. This results in significant turn-on losses for all of the four transistors.

The above losses can be significantly reduced by increasing the base current to reduce the transistor turn-on time and by introducing the commutating circuits shown in Fig. 9. When $Q2$ starts to turn on, V_s will appear across L_{c1} and L_{c2} instead of v_{CE2}. This arrangement results in much lower transistor turn-on losses as can be

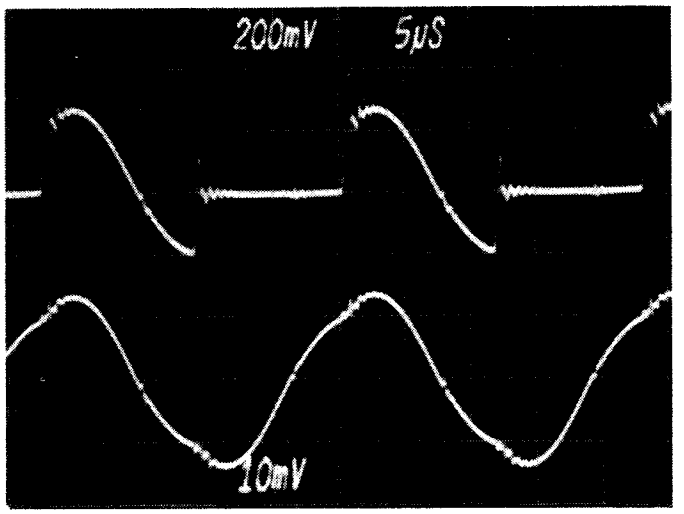

Fig. 8. Upper trace: Current in one diode-transistor pair in Fig. 1. Lower trace: Load current I_0. Scale: 2 A/div, 5 μs/div.

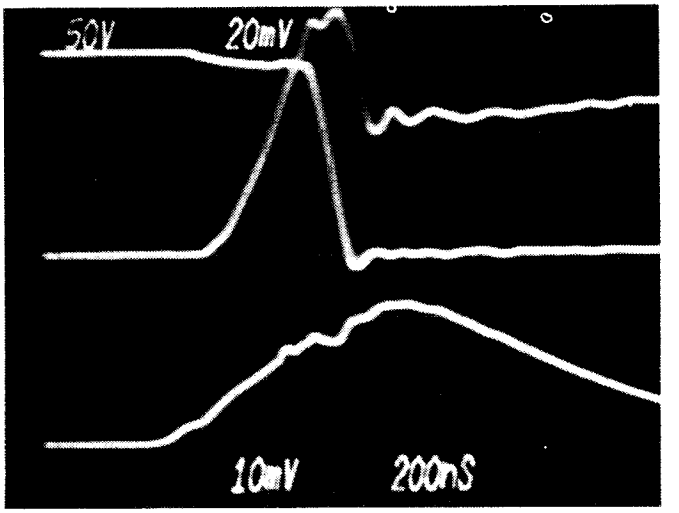

Fig. 10. Switching transistor waveforms at turn-on without commutating circuit. Upper trace: Collector-emitter voltage v_{CE} (falling), 50V/div. Collector current i_C (rising), 1A/div. Lower trace: Base current i_B, 200 mA/div. Time scale: 200 ns/div.

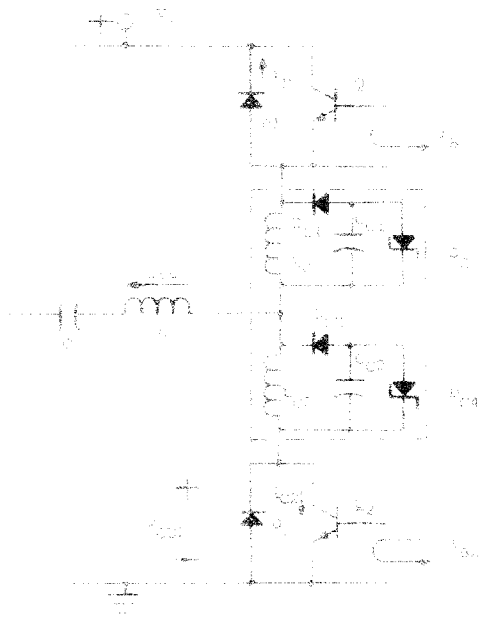

Fig. 9. Detailed schematic showing commutating inductors for 50 kHz full-bridge converter. $C = 0.016\ \mu F$, $L = 592\mu H$, $L_1 = L_2 = 12\ \mu H$. $D_1 = D_2 = 1N4935$, $D_3 = D_4 = 1N4751$.

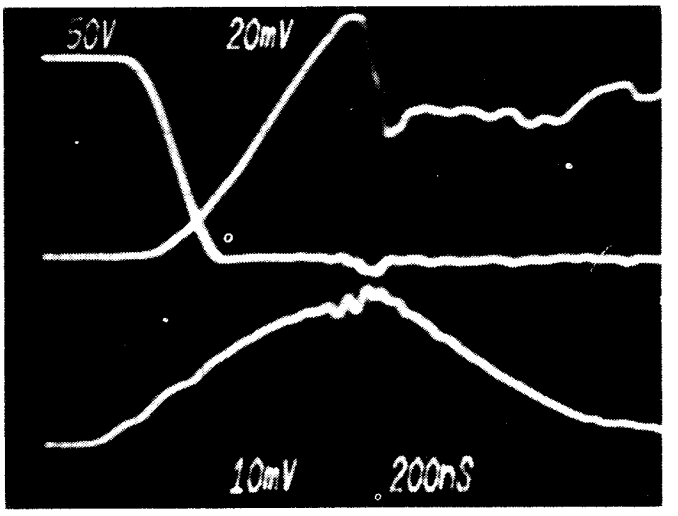

Fig. 11. Switching transistor waveforms at turn-on with commutating circuit shown in Fig. 9. Upper traces: Collector-emitter voltage v_{CE} (falling), 50v/div. Collector current i_C(rising), 1A/div. Lower trace: Base current i_B, 200 mA/div. Time scale: 200 ns/div.

seen from the i_C and v_{CE} waveforms in Fig. 11, L_1 is quite small in comparison to the main inductor L so it has only a minor effect on the calculated results. However this effect can be included in an approximate manner by using the new total series inductance, $L + 2L_1$ in place of L. The remaining components in the commutating circuit are to prevent excessive v_{CE} following the switching intervals.

SUMMARY

The equations and normalized parametric curves provide a comprehensive model for the full-bridge converter, just as those presented earlier in [1] did for the half-bridge circuit. Curves of this type can be a very effective design tool and give a quick indication of how changes in various parameters will affect circuit performance. The calculated results also show good agreement with measurements taken from a 50 kHz converter, as long as circuit losses are included with the output power.

REFERENCES

[1] King, R, and Stuart, T. (1981)
A normalized model for the half bridge series resonant converter.
IEEE Transactions on Aerospace and Electronic Systems, Mar. 1981, *AES-17*, 190-198.

[2] Schwarz, F.C. (1970)
A method of resonant current pulse modulation for power converters.
IEEE Transactions on Industrial Electronics and Control Instrumentation, May 1970, *IECI-17*, 209-221.

[3] Biess, J., Inouye, L., and Shank, J.H. (1974)
High voltage series resonant inverter ion engine screen supply.
Proceedings of the 1974 IEEE Power Electronics Specialists Conference, Bell Laboratories, Murray Hill, NJ, June 1974, 97-105.

[4] Schwarz, F.C., and Klaasens, J.B. (1975)
A controllable secondary multikilowatt dc current source with constant maximum power factor in its 3 phase supply line.
In *Proceedings of the 1975 IEEE Power Electronics Specialists Conference*, 1975, 205-215.

[5] Schwarz, F.C. (1976)
An improved method of resonant current pulse modulation for power converters.
IEEE Transactions on Industrial Electronics and Control Instrumentation, May 1976, *IECI-23*, 133-141.

[6] Kittl, E. (1977)
Transient waveform analysis of switching converter.
Technical Report ECOM-4493, U.S. Army Electronics Command, DRSEL-TL-PE, Fort Monmouth, NJ, Apr. 1977.

[7] Schwarz, F.C., and Klaasens, J.B. (1978)
A 95 percent efficient 1 kW dc converter with an internal frequency of 50 KHz.
IEEE Transactions on Industrial Electronics and Control Instrumentation, Nov. 1978, *IECI-25*, 326-333.

[8] Dougherty, M.P. (1979)
A series resonant inverter simulation using super-sceptre.
In *Proceedings of the National Aerospace and Electronics Conference*, Dayton, OH, May 1979, 517-524.

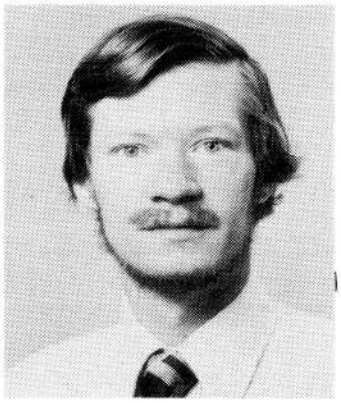

Roger J. King was born in Toledo, OH, on September 28, 1950. He received the B.S.E.E. and the M.S.E.E. degrees from the University of Toledo in 1972 and 1975, respectively.

From 1976 to 1978 he worked as a Biomedical Engineer at the University of West Virginia and at the Medical College of Ohio, designing analog instrumentation. He is presently a Graduate Research Assistant at the University of Toledo, involved in power electronics research and working towards the Ph.D degree.

Mr. King is a member of Eta Kappa Nu and Tau Beta Pi.

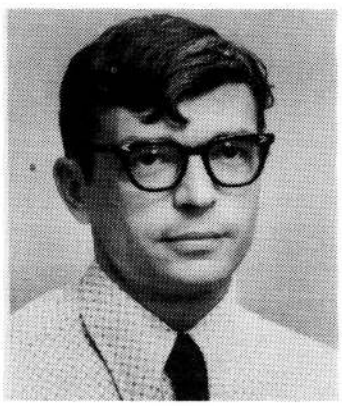

Thomas S. Stuart (S'69—M'72—SM'80) was born in Bloomington, IN, on February 6, 1941. He received the B.S.E.E. degree from the University of Illinois, Urbana, and the M.E. and the Ph.D. degrees from Iowa State University, Ames, in 1963, 1969, and 1972, respectively.

He is presently an Associate Professor of Electrical Engineering at the University of Toledo, Toledo, OH, where he is engaged in teaching and research. His primary interests are in electrical power systems and power electronics. Prior to joining Toledo in 1975, he taught within the Department of Electrical and Computer Engineering at Clarkson College of Technology, Potsdam, NY. He has also worked in the areas of power electronics and circuit design for Collins Radio Company, Honeywell, Inc., and Martin Company.

Dr. Stuart is a registered Professional Engineer in the State of Ohio and is a member of Eta Kappa Nu, Sigma Xi, and Phi Kappa Phi.